

Unearthing the soil carbon food web with high resolution DNA-SIP

Ashley N Campbell and Charles Pepe-Ranney * † ‡, Chantal Koechli, Sean Berthrong, and Daniel H Buckley ‡

* These authors contributed equally to the manuscript and should be considered co-first authors, † Department of Microbiology, Cornell University, New York, USA, and ‡ Department of Crop and Soil Sciences, Cornell University, New York, USA

Submitted to Proceedings of the National Academy of Sciences of the United States of America

Abstract

We describe an approach for identifying microbial contributions to soil C cycling using nucleic acid stable isotope probing (SIP) coupled with next generation sequencing. ^{13}C -xylose or ^{13}C -cellulose were chosen to carry the isotopic label for DNA-SIP. Microcosm DNA was interrogated for ^{13}C incorporation at days 1, 3, 7, 14 and 30. Incorporation of ^{13}C from xylose into microcosm DNA was observed at days 1, 3, and 7, while incorporation of ^{13}C from cellulose peaked at day 14 and was maintained through day 30. From approximately 6,000 OTUs detected, a total of 49 and 63 unique OTUs assimilated ^{13}C from xylose and cellulose into DNA, respectively. Xylose assimilating OTUs were more abundant in the microcosm community than cellulose assimilating OTUs, while cellulose OTUs demonstrated a greater substrate specificity than xylose OTUs.

monolayer | structure | x-ray reflectivity | molecular electronics

Abbreviations: SAM, self-assembled monolayer; OTS, octadecyl-trichlorosilane

Significance

We have limited understanding of soil carbon (C) cycling yet soil contains a large fraction of the global C pool. Microorganisms mediate most soil C cycling but have proven difficult to study due to the complexity of soil C biochemistry and the wide range of soil microorganisms participating in C reactions. We demonstrate temporal C use dynamics in discrete soil microbial taxa. Furthermore, we identified novel microorganisms involved in cellulose decomposition, the most globally abundant biopolymer. Further application of the method demonstrated in this paper will identify microbial taxa that mediate soil C transformations for more substrates and soils and increase our understanding of global soil C cycling.

Introduction

Excluding plant biomass, there are 2,300 Pg of carbon (C) stored in soils worldwide which accounts

for ~80% of the global terrestrial C pool [1, 2]. When organic C from plants reaches soil it is degraded by fungi, archaea, and bacteria. The majority of plant biomass C in soil is respired and produces 10 times more CO_2 annually than anthropogenic emissions [3]. Global changes in atmospheric CO_2 , temperature, and ecosystem nitrogen inputs are expected to impact soil C input [4]. Current climate change models concur on atmospheric and oceanic but not terrestrial C predictions [5]. Contrasting terrestrial C model predictions reflect how little is known about soil C cycling. Inconsistencies in terrestrial modeling could be improved by elucidating the relationship between dissolved organic C and soil microbial community composition [6].

To establish the relationship between community structure and soil function we must identify the *in situ* activity of specific soil microbes [7]. An estimated 80-90% of soil C cycling is mediated by microorganisms [8, 9] but exploring soil C processing is challenging due to soil's heterogeneous nature. The majority of microorganisms resist cultivation in the laboratory. Stable-isotope probing (SIP) links genetic identity and activity without cultivation and has been used to expand our knowledge of microbial contributions to biogeochemical processes [10]. Successful applications of SIP have identified organisms which mediate processes performed by a narrow set of functional guilds such as methanogens [11] but SIP has been less applicable in soil C cycling studies due to limitations in resolving power as a result of simultaneous labeling of many different organisms. High throughput

Reserved for Publication Footnotes

DNA sequencing technology, however, has enabled exploration of complex soil C-cycling patterns via SIP.

A temporal activity cascade occurs in natural microbial communities during plant biomass degradation in which labile C is degraded before polymeric C [12, 13]. This study’s aim was to observe C assimilation dynamics in the soil microbial community. Our experimental approach included the addition of a soil organic matter (SOM) simulant to soil microcosms where a single C component was substituted for its ^{13}C equivalent. Parallel incubations of soils amended with this C mixture allowed us to observe how different C substrates move through the soil microbial community. In this study we used ^{13}C -xylose and ^{13}C -cellulose as a proxy for labile and polymeric C, respectively, and coupled nucleic acid SIP with high throughput DNA sequencing. Amplicon sequencing of 16S rRNA genes from gradient fractions of multiple density gradients made it possible to track C assimilation by hundreds of soil taxa.

Results

We observed C use dynamics in an agricultural soil microbial community by conducting a nucleic acid SIP experiment wherein xylose or cellulose carried the isotopic label. We set up three soil microcosm series. Each microcosm was amended with a C substrate mixture that included cellulose and xylose. The C substrate mixture approximated the C composition of fresh plant biomass. The same mixture was added to all microcosms, however, for each series except the control, xylose or cellulose was substituted for its ^{13}C counterpart. Microcosms are identified in figures by the following code: “13CXPS” refers to the amendment with ^{13}C -xylose (^{13}C Xylose Plant Simulant), “13CCPS” refers to the ^{13}C -cellulose amendment and “12CCPS” refers to the amendment that only contained ^{12}C (i.e. control). 5.3 mg C substrate mixture per gram of soil was added to each microcosm representing 18% of the soil C. The mixture included 0.42 mg xylose-C and 0.88 mg cellulose-C per gram soil. Microcosms were harvested at days 1, 3, 7, 14 and 30 during a 30 day incubation. ^{13}C -xylose assimilation peaked immediately and tapered over the 30 day incubation whereas ^{13}C -cellulose assimilation peaked two weeks after amendment additions (Figure 1, Figure S1). See Supplemental Note XX for sequencing and density fractionation statistics.

Soil microcosm microbial community changes with time.

Changes in the bulk soil microcosm microbial community structure and membership correlated significantly with incubation time (Figure S2B, p-value 0.23, R^2 0.63, Adonis test [14]).

The identity of the ^{13}C -labeled substrate added to the microcosms did not significantly correlate with bulk soil community structure and membership (p-value 0.35). Additionally, microcosm beta diversity was significantly less than gradient fraction beta diversity (Figure S2, p-value 0.003, “betadisper” function R Vegan package [15, 16], Figure S2). Twenty-nine OTUs significantly changed in relative abundance with time (“BH” adjusted p-value <0.10, [17]) and of these 29 OTUs, 14 were labeled substrate responders (Figure S3). If sequences were grouped by taxonomic annotations at the class level, only four classes significantly changed in abundance, *Bacilli* (decreased), *Flavobacteria* (decreased), *Gammaproteobacteria* (decreased) and *Herpetosiphonales* (increased) (Figure S4).

Responder abundances summed at phylum level increased for ^{13}C -cellulose (Figure S5) whereas ^{13}C -xylose responder abundances summed at the phylum level decreased over time for *Firmicutes*, *Bacteroidetes*, *Actinobacteria* and *Proteobacteria* although *Proteobacteria* spiked at day 14 (Figure S5).

OTUs that assimilated ^{13}C into DNA. Within the first 7 days of incubation approximately 63% of ^{13}C -xylose was respired and only an additional 6% more was respired from day 7 to 30. At day 30, 30% of the ^{13}C from xylose remained. An average 16% of the ^{13}C -cellulose added was respired within the first 7 days, 38% by day 14, and 60% by day 30.

We refer to OTUs that putatively incorporated ^{13}C into DNA originally from an isotopically labeled substrate as substrate “responders” (see Supplemental Note XX for “response” criteria). There were X, X, X, X ^{13}C -xylose responders at days 1, 3, 7, 14, 30, respectively (Figure S1). At day 1, 84% of ^{13}C -xylose responsive OTUs belonged to *Firmicutes*, 11% to *Proteobacteria* and 5% to *Bacteroidetes*. *Firmicutes* responders decreased from 16 OTUs at day 1 to one OTU at day 3 while *Bacteroidetes* responders increased from one OTU at day 1 to 12 OTUs at day 3. The remaining day 3 responders are members of the *Proteobacteria* (26%) and the *Verrucomicrobia* (5%). Day 7 responders were 53% *Actinobacteria*, 40% *Proteobacteria*, and 7% *Firmicutes*. The identities of ^{13}C -xylose responders changed with time. The numerically dominant ^{13}C -xylose responder phylum shifted from *Firmicutes* to *Bacteroidetes* and then to *Actinobacteria* across days 1, 3 and 7 (Figure 2, Figure 3).

Only 2 and 5 OTUs had incorporated ^{13}C from ^{13}C -cellulose at days 3 and 7, respectively. At days 14 and 30, 42 and 39 OTUs incorporated ^{13}C from ^{13}C -cellulose into biomass (Figure S1). A *Celvibrio* and *Sandaracinaceae* OTU assimilated ^{13}C

from ^{13}C -cellulose at day 3. Day 7 ^{13}C -cellulose responders included the same *Cellvibrio* responder as day 3, a *Verrucomicrobia* OTU and three *Chloroflexi* OTUs. 50% of Day 14 responders belong to *Proteobacteria* (66% Alpha-, 19% Gamma-, and 14% Beta-) followed by 17% *Planctomycetes*, 14% *Verrucomicrobia*, 10% *Chloroflexi*, 7% *Actinobacteria* and 2% cyanobacteria. *Bacteroidetes* OTUs began to incorporate ^{13}C from cellulose at day 30 (13% of day 30 responders). Other day 30 responding phyla included *Proteobacteria* (30% of day 30 responders; 42% Alpha-, 42% Delta, 8% Gamma-, and 8% Beta-), *Planctomycetes* (20%), *Verrucomicrobia* (20%), *Chloroflexi* (13%) and cyanobacteria (3%). *Proteobacteria*, *Verrucomicrobia*, and *Chloroflexi* had relatively high numbers of responders with strong response across multiple time points (Figure 2).

See Supplemental Note XX for further analysis of ^{13}C -responsive OTUs at greater taxonomic resolution.

Ecological strategies of ^{13}C responders. ^{13}C -xylose responders are generally more abundant members based on relative abundance in bulk DNA SSU rRNA gene content than ^{13}C -cellulose responders (Figure 4, p-value 0.00028, Wilcoxon Rank Sum test). However, both abundant and rare OTUs responded to ^{13}C -xylose and ^{13}C -cellulose (Figure 4). Two ^{13}C -cellulose responders were not found in any bulk samples (“OTU.862” and “OTU.1312”, Table S1). Of the 10 most abundant responders, 8 are ^{13}C -xylose responders and 6 of these 8 are consistently among the 10 most abundant OTUs in bulk samples.

Cellulose responders exhibited a greater shift in buoyant density (BD) than xylose responders in response to isotope incorporation (Figure S6, Figure 4, p-value 1.8610×10^{-6} , Wilcoxon Rank Sum test). ^{13}C -cellulose responders shifted on average 0.0163 g mL^{-1} (sd 0.0094) whereas xylose responders shifted on average 0.0097 g mL^{-1} (sd 0.0094). For reference, 100% ^{13}C DNA BD is 0.04 g mL^{-1} greater than the BD of its ^{12}C counterpart. DNA BD increases as its ratio of ^{13}C to ^{12}C increases. An organism that only assimilates C into DNA from a ^{13}C isotopically labeled source, will have a greater ^{13}C : ^{12}C ratio in its DNA than an organism utilizing a mixture of isotopically labeled and unlabeled C sources (see supplemental note XX).

^{13}C -xylose responder estimated *rrn* gene copy number was inversely related time of first response (p-value 2.02×10^{-15} , Figure S7). OTUs that first respond at later time points have fewer estimated *rrn* copy number than OTUs that first respond earlier (Figure S7).

We assessed phylogenetic clustering of ^{13}C -responsive OTUs with the Nearest Taxon In-

dex (NTI) and the Net Relatedness Index (NRI). Briefly, positive NRI and NTI with corresponding low P-values indicates deep phylogenetic clustering whereas negative NRI with high P-values indicates taxa are overdispersed against the null model CITE. NRI and P-values for substrate responder groups suggest ^{13}C -xylose responders are overdispersed (NRI: -1.33, P: 0.90) while cellulose responders are clustered (NRI: 4.49, P: 0.001). Nearest taxon indices (NTI) show that both ^{13}C -cellulose and ^{13}C -xylose responders are clustered near the tips of the tree (NTI: 1.43 (P: 0.072), 2.69 (P: 0.001), respectively).

Discussion

Pure culture based studies have historically driven soil microbial ecology research but cultured isolates have not captured *in situ* numerically abundant genera [18]. DNA-SIP can characterize functional roles for thousands of phylotypes in a single experiment without cultivation. We identified 104 OTUs in an agricultural soil that incorporated ^{13}C from xylose and/or cellulose into biomass and characterized substrate specificity and C-cycling dynamics for these soluble and polymeric C degraders. Included in ^{13}C -xylose and ^{13}C -cellulose responsive OTUs were members of cosmopolitan yet functionally uncharacterized soil phylogenetic groups such as *Verrucomicrobia*, *Planctomycetes* and *Chloroflexi*.

Microbial response to isotopic labels. We propose that C added to soil microcosms in this experiment took the following path through the microbial food web (Figure S8): First, labile C such as xylose was assimilated by fast-growing opportunistic *Firmicutes* spore formers. The remaining labile C and new biomass C was assimilated in succession by slower growing *Bacteroidetes*, *Actinobacteria* and *Proteobacteria* phylotypes that were either tuned to lower C substrate concentrations, were predatory bacteria (e.g. *Agromyces*), and/or were specialized for consuming viral lysate. C from polymeric substrates entered the bacterial community after 14 days. Canonical cellulose degrading bacteria such as *Cellvibrio* degraded cellulose but uncharacterized lineages in the *Chloroflexi*, *Planctomycetes* and *Verrucomicrobia*, specifically the *Spartobacteria*, were also significant contributors to cellulose decomposition.

Ecological strategies of soil microorganisms participating in the decomposition of organic matter. We assessed the ecology of ^{13}C -responsive OTUs by estimating the *rrn* gene copy number and the BD shift upon labeling for each OTU. *rrn* gene copy number correlates positively with growth rate

[19] and BD shift is indicative of substrate specificity (see results). Ecological metrics suggest ¹³C-cellulose responsive OTUs grow slower (Figure 4, Figure S7), have greater substrate specificity (Figure 4), and are generally lower abundance than ¹³C-xylose responsive OTUs (Figure 4). The higher abundance of xylose responders may also be in part due to higher *rrn* gene copy number. ¹³C-xylose responsive OTU *rrn* gene copy number correlated inversely with the time at which the OTU was first found to incorporate ¹³C into DNA (Figure 4, Figure S7) suggesting fast-growing microbes assimilated ¹³C from xylose before slow growers. Labile C responder ecological strategies were more varied than polymeric C responder ecological strategies perhaps because ¹³C labeled microorganisms did not primarily assimilate xylose but became labeled via predatory interactions and/or are saprophytes.

NRI values have been used to assess soil OTUs categorized by clustering relative abundance profiles in response to wet up (CITE Firestone and Wallenstein). Ecological groups defined by response to repeated wet up over XX weeks varied in phylogenetic clustering whereas groups defined by assessing relative abundance patterns within a single wet up event were largely phylogenetically clustered (CITE). We found that cellulose and xylose responders are clustered and overdispersed, respectively. This suggests that the ability to degrade cellulose is tied to phylogeny. Overdispersion, as we saw for the ¹³C-xylose responsive OTUs, may be indicative of a trait that can be transferred between species and/or a trait that is broadly distributed phylogenetically. Although, it's not clear if most ¹³C-xylose responsive organisms were all labeled as a result of primary xylose assimilation (see below), and therefore it's not clear if ¹³C-xylose responsive OTUs in this experiment constitute a single ecologically meaningful group or multiple groups.

Implications for soil C cycling models. Land management, climate, pollution and disturbance can all influence soil community composition [20] which in turn can influence soil biogeochemical process rates (e.g. [21]). Assessing functional group diversity and establishing identities of functional group members is an important step in predicting how biogeochemical process rates can change with community composition [20, 22]. We highlight three key results in our study with implications for models of soil C cycling:

- labile and polymeric C decomposers functional guilds are similar in diversity,
- labile C cycling may include significant trophic interactions, and

- soil biomass does not respond *en masse* to C additions.

Biogeochemical processes carried out by few taxa or “narrow” guilds are influenced more significantly by changes in community composition than processes carried out by greater numbers of taxa [20, 22]. Labile and recalcitrant C decomposition are considered to be carried out by “broad” and “narrow” functional guilds, respectively [20, 22]. However, the diversity of active labile C and insoluble, polymeric C decomposers in soil has not been directly quantified. Our results conflict with the established paradigm of decreasing diversity in guilds responsible transforming more recalcitrant C substrates. We found more OTUs responded to ¹³C-cellulose, 63, than ¹³C-xylose, 49, and it is possible that many ¹³C-xylose responders are predatory bacteria as opposed to primary labile C degraders (see below). Both ¹³C-cellulose and ¹³C-xylose responders were largely clustered at taxonomic levels broader than the OTUs established in this study (Figure S9) with *Proteobacteria* ³⁸⁵ ¹³C-responders being an exception for both cellulose and xylose responders. When grouped at greater phylogenetic depth ¹³C-responders can be distributed into a few clades (Figure S9). This suggests both cellulose and xylose decomposition are “narrow” processes.

The activity succession from *Firmicutes* to *Bacteroidetes* and finally *Actinobacteria* in response to ¹³C-xylose addition marks a trophic cascade and/or functional groups tuned to different resource concentrations. *Actinobacteria* (e.g. *Agromyces*) and *Bacteroidetes* have been previously implicated as predatory soil bacteria [23]. Further, the activity peak of *Bacteroidetes* and *Actinobacteria* occurred with a concomitant decrease in *Firmicutes* ³⁹⁵ ¹³C-xylose responder relative abundance. Considering that *Agromyces* and certain *Bacteroidetes* types are likely soil predators [23, 24] one parsimonious hypothesis for ¹³C-labelling of *Bacteroidetes* and *Actinobacteria* with a corresponding decrease in abundance of ¹³C-labeled *Firmicutes* is that the *Bacteroidetes* and *Actinobacteria* fed on the ¹³C-labeled *Firmicutes*. If the temporal dynamics of ¹³C-xylose incorporation are due to trophic interactions, our results suggest that many, if not most, fast-growing labile C degraders are consumed by predatory bacteria. Hence, predatory interactions between soil bacteria may be of importance for modelling soil C turnover though intra-bacteria trophic interactions in soil C cycling are often not considered (e.g. [25]).

It has been proposed that incorporating soil microbial community structure into biogeochemical process models will improve predictions of global C fluxes in response to climate change [20] but first we need to understand the functional roles

of soil microorganisms and the diversity of functional guilds. We demonstrate the soil functional guilds that participated in xylose and cellulose decomposition in our microcosms. These functional guilds were non-overlapping in membership and represented a small fraction of total soil community diversity (Figure 5). Of 104 ^{13}C -responders only 8 responded to both cellulose and xylose. Also, while we observed nearly 6,000 OTUs the number of conclusively active OTUs in xylose and cellulose decomposition were 49 and 63, respectively. Our results suggest that ecosystem C cycling models may need to assess parameters independently for C-cycling functional guilds as functional guilds are largely non-overlapping with respect to microbial membership and each functional guild represents a small fraction of overall soil microbial diversity.

Conclusion. Microorganisms sequester atmospheric C and respire SOM influencing climate change on a global scale but we do not know which microorganisms carry out specific soil C transformations. In this experiment microbes from uncharacterized yet ubiquitous soil lineages participated in cellulose decomposition. Cellulose C degraders included members of the *Verrucomicrobia* (*Spartobacteria*), *Chloroflexi*, *Bacteroidetes* and *Planctomycetes*. *Spartobacteria* in particular are globally cosmopolitan soil microorganisms and are often the most abundant *Verrucomicrobia* order in soil [26]. Our results also suggest that members of the *Bacteroidetes* and *Actinobacteria* act in the cascade of labile, soluble C through soil trophic levels possibly as predators. Both points illustrate the complexity of soil C dynamics and fate. The largely phylogenetically coherent ecological groups observed in this study suggest that soil C dynamics are tied to phylogenetic composition.

Methods

Additional information on sample collection and analytical methods is provided in SI Materials and Methods.

Twelve soil cores (5 cm diameter x 10 cm depth) were collected from six random sampling locations within an organically managed agricultural field in Penn Yan, New York. Soils were pretreated by sieving (2 mm), homogenizing sieved soil, and pre-incubating 10 g of dry soil weight in flasks for 2 weeks. Soils were amended with a 5.3 mg g soil $^{-1}$ carbon mixture; representative of natural concentrations [27]. Mixture contained 38% cellulose, 23% lignin, 20% xylose, 3% arabinose, 1% galactose, 1% glucose, and 0.5% mannose by mass, with the remaining 13.5% mass composed of an amino acid (in-house made replica of Teknova C0705) and basal salt mixture (Murashige and Skoog, Sigma Aldrich M5524). Three parallel treatments were

performed; (1) unlabeled control,(2) ^{13}C -cellulose, (3) ^{13}C -xylose (98 atom% ^{13}C , Sigma Aldrich). Each treatment had 2 replicates per time point (n = 4) except day 30 which had 4 replicates; total microcosms per treatment n = 12, except ^{13}C -cellulose which was not sampled at day 1, n = 10. Other details relating to substrate addition can be found in SI. Microcosms were sampled destructively (stored at -80°C until nucleic acid processing) at days 1 (control and xylose only), 3, 7, 14, and 30.

Nucleic acids were extracted using a modified Griffiths protocol [28]. To prepare nucleic acid extracts for isopycnic centrifugation as previously described [29], DNA was size selected (>4kb) using 1% low melt agarose gel and β -agarase I enzyme extraction per manufacturers protocol (New England Biolab, M0392S). For each time point in the series isopycnic gradients were setup using a modified protocol [30] for a total of five ^{12}C -control, five ^{13}C -xylose, and four ^{13}C -cellulose microcosms. A density gradient (average density 1.69 g mL $^{-1}$) solution of 1.762 g cesium chloride (CsCl) mL $^{-1}$ in gradient buffer solution (pH 8.0 15 mM Tris-HCl, 15 mM EDTA, 15 mM KCl) was used to separate ^{13}C -enriched and ^{12}C -nonenriched DNA. Each gradient was loaded with approximately 5 μg of DNA and ultracentrifuged for 66 h at 55,000 rpm and room temperature (RT). Fractions of ~100 μL were collected from below by displacing the DNA-CsCl-gradient buffer solution in the centrifugation tube with water using a syringe pump at a flow rate of 3.3 $\mu\text{L s}^{-1}$ [31] into AcroprepTM 96 filter plate (Pall Life Sciences 5035). The refractive index of each fraction was measured using a Reichart AR200 digital refractometer modified as previously described [29] to measure a volume of 5 μL . Then buoyant density was calculated from the refractive index as previously described [29] (see also SI). The collected DNA fractions were purified by repetitive washing of Acroprep filter wells with TE. Finally, 50 μL TE was added to each fraction then resuspended DNA was pipetted off the filter into a new microfuge tube.

For every gradient, 20 fractions were chosen for sequencing between the density range 1.67-1.75 g mL $^{-1}$. Barcoded 454 primers were designed using 454-specific adapter B, 10 bp barcodes [32], a 2 bp linker (5'-CA-3'), and 806R primer for reverse primer (BA806R); and 454-specific adapter A, a 2 bp linker (5'-TC-3'), and 515F primer for forward primer (BA515F). Each fraction was PCR amplified using 0.25 μL 5 U μl^{-1} AmpliTaq Gold (Life Technologies, Grand Island, NY; N8080243), 2.5 μL 10X Buffer II (100 mM Tris-HCl, pH 8.3, 500 mM KCl), 2.5 μL 25 mM MgCl $_2$, 4 μL 5 mM dNTP, 1.25 μL 10 mg mL $^{-1}$ BSA, 0.5 μL 10 μM BA515F, 1 μL 5 μM BA806R, 3 μL H $_2$ O,

- 535 10 μ L 1:30 DNA template) in triplicate. Samples were normalized either using Pico green quantification and manual calculation or by SequalPrep™ normalization plates (Invitrogen, Carlsbad, CA; A10510), then pooled in equimolar concentrations. 595
- 540 Pooled DNA was gel extracted from a 1% agarose gel using Wizard SV gel and PCR clean-up system (Promega, Madison, WI; A9281) per manufacturer's protocol. Amplicons were sequenced on Roche 454 FLX system using titanium chemistry at Selah Genomics (formerly EnGenCore, Columbia, SC)
- 545
- ## References
1. Amundson R (2001) The carbon budget in soils. *Annu Rev Earth Planet Sci* 29(1): 535–562.
 2. Batjes N-H (1996) Total carbon and nitrogen in the soils of the world. *European Journal of Soil Science* 47(2): 151–163.
 3. Chapin F (2002) Principles of terrestrial ecosystem ecology.
 4. Groenigen K-J, Graaff M-A, Six J, Harris D, Kuikman P, Kessel C (2006) The impact of elevated atmospheric CO₂ on soil C and N dynamics: a meta-analysis. *Managed Ecosystems and CO₂* (Springer Science, Berlin Heidelberg), pp 373–391.
 5. Friedlingstein P, Cox P, Betts R, Bopp L, von W-B, Brovkin V, et al. (2006) Climate–carbon cycle feedback analysis: Results from the C4 model intercomparison. *J Climate* 19(14): 3337–3353.
 6. Neff J-C, Asner G-P (2001) Dissolved organic carbon in terrestrial ecosystems: synthesis and a model. *Ecosystems* 4(1): 29–48.
 7. O'Donnell A-G, Seasman M, Macrae A, Waite I, Davies J-T (2002) Plants and fertilisers as drivers of change in microbial community structure and function in soils. *Interactions in the Root Environment: An Integrated Approach* (Springer, Netherlands), pp 135–145.
 8. Coleman D-C, Crossley D-A (1996) Fundamentals of Soil Ecology.
 9. Nannipieri P, Ascher J, Ceccherini M-T, Landi L, Pietramellara G, Renella G (2003) Microbial diversity and soil functions. *European Journal of Soil Science* 54(4): 655–670.
 10. Chen Y, Murrell J-C (2010) When metagenomics meets stable-isotope probing: progress and perspectives. *Trends Microbiol* 18(4): 157–163.
 11. Lu Y (2005) In situ stable isotope probing of methanogenic archaea in the rice rhizosphere. *Science* 309(5737): 1088–1090.
 12. Hu S, van Bruggen A-HC (1997) Microbial dynamics associated with multiphasic decompo-
 - 550 sition of ¹⁴C-Labeled Cellulose in Soil. *Microb Ecol* 33(2): 134–143.
 13. Rui J, Peng J, Lu Y (2009) Succession of bacterial populations during plant residue decomposition in rice field soil. *Appl Environ Microbiol* 75(14): 4879–4886.
 14. Anderson M-J (2001) A new method for non-parametric multivariate analysis of variance. *Austral Ecology* 26(1): 32–46.
 15. Anderson M-J, Ellingsen K-E, McArdle B-H (2006) Multivariate dispersion as a measure of beta diversity. *Ecology Letters* 9(6): 683–693.
 16. Oksanen J, Kindt R, Legendre P, OHara B, Stevens M-HH, Oksanen M-J, et al. (2007) The vegan package.
 17. Benjamini Y, Hochberg Y (1995) Controlling the false discovery rate: a practical and powerful approach to multiple testing. *Journal of the Royal Statistical Society, Series B* 57(1): 289–300.
 18. Janssen P-H (2006) Identifying the dominant soil bacterial taxa in libraries of 16S rRNA and 16S rRNA genes. *Appl Environ Microbiol* 72(3): 1719–1728.
 19. Klappenbach J, Saxman P, Cole J, Schmidt T (2001) rrndb: the Ribosomal RNA Operon Copy Number Database.. *Nucleic Acids Res* 29(1): 181–184.
 20. McGuire K-L, Treseder K-K (2010) Microbial communities and their relevance for ecosystem models: Decomposition as a case study. *Soil Biology and Biochemistry* 42(4): 529–535.
 21. Berlemont R, Allison S-D, Weihe C, Lu Y, Brodie E-L, Martiny J-BH, et al. (2014) Cellulolytic potential under environmental changes in microbial communities from grassland litter. *Front Microbiol* 5: 639.
 22. Schimel J (1995) Ecosystem consequences of microbial diversity and community structure. *Arctic and alpine biodiversity: patterns, causes and ecosystem consequences*, , eds. III P-DFSC, Körner P-DC, Ecological Studies (Springer, Berlin Heidelberg), pp 239–254.
 23. Lueders T, Kindler R, Miltner A, Friedrich M-W, Kaestner M (2006) Identification of bacterial micropredators distinctively active in a soil microbial food web. *Appl Environ Microbiol* 72(8): 5342–5348.
 24. Casida L-E (1983) Interaction of Agromyces ramosus with Other Bacteria in Soil.. *Appl Environ Microbiol* 46(4): 881–888.
 25. Moore J-C, Walter D-E, Hunt H-W (1988) Arthropod Regulation of Micro- and Mesobiota in Below-Ground Detrital Food Webs. *Annu Rev Entomol* 33(1): 419–435.
 26. Bergmann G-T, Bates S-T, Eilers K-G, Lauber C-L, Caporaso J-G, Walters W-A, et al. (2011) The under-recognized dominance of Verru-



- 650 comicrobia in soil bacterial communities. *Soil Biology and Biochemistry* 43(7): 1450–1455.
27. Schneckenberger K, Demin D, Stahr K, Kuzyakov Y (2008) Microbial utilization and mineralization of ^{14}C glucose added in six orders of concentration to soil. *Soil Biology and Biochemistry* 40(8): 1981–1988.
- 655 28. Griffiths R-I, Whiteley A-S, O'Donnell A-G, Bailey M-J (2000) Rapid method for coextraction of DNA and RNA from natural environments for analysis of ribosomal DNA- and rRNA-based microbial community composition. *Appl Environ Microbiol* 66(12): 5488–5491.
- 660 29. Buckley D-H, Huangyutitham V, Hsu S-F, Nelson T-A (2007) Stable isotope probing with ^{15}N achieved by disentangling the effects of genome G+C content and isotope enrichment on dna Density. *Appl Environ Microbiol* 73(10): 3189–3195.
30. Neufeld J-D, Vohra J, Dumont M-G, Lueders T, Manefield M, Friedrich M-W, et al. (2007) DNA stable-isotope probing. *Nature Protocols* 2(4): 860–866.
31. Manefield M, Whiteley A-S, Griffiths R-I, Bailey M-J (2002) RNA Stable isotope probing a novel means of linking microbial community function to phylogeny. *Appl Environ Microbiol* 68(11): 5367–5373.
32. Hamady M, Walker J-J, Harris J-K, Gold N-J, Knight R (2008) Error-correcting barcoded primers for pyrosequencing hundreds of samples in multiplex. *Nat Meth* 5(3): 235–237.

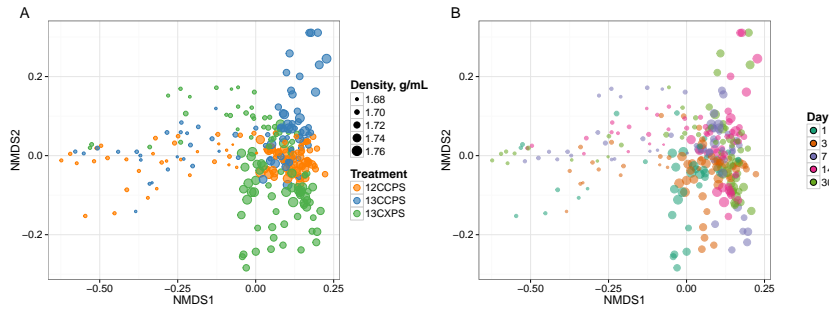


Fig. 1. NMDS analysis from weighted unifrac distances of 454 sequence data from SIP fractions of each treatment over time. Twenty fractions from a CsCl gradient fractionation for each treatment at each time point were sequenced (Fig. S1). Each point on the NMDS represents the bacterial composition based on 16S sequencing for a single fraction where the size of the point is representative of the density of that fraction and the colors represent the treatments (A) or days (B).

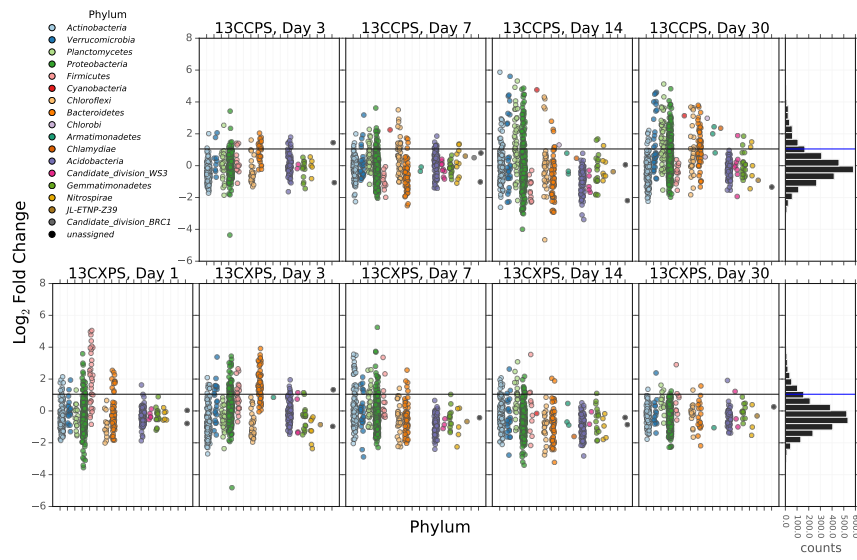


Fig. 2. Log₂ fold change of ¹³C-responders in cellulose treatment (top) and xylose treatment (bottom). Log₂ fold change is based on the relative abundance in the experimental treatment compared to the control within the density range 1.7125–1.755 g ml⁻¹. Taxa are colored by phylum. ‘Counts’ is a histogram of log₂ fold change values.

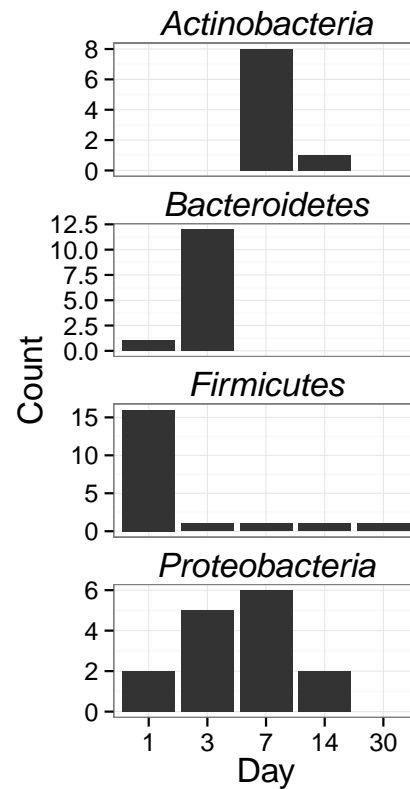


Fig. 3. Counts of ^{13}C -xylose responders in the *Actinobacteria*, *Bacteroidetes*, *Firmicutes* and *Proteobacteria* at days 1, 3, 7 and 30.

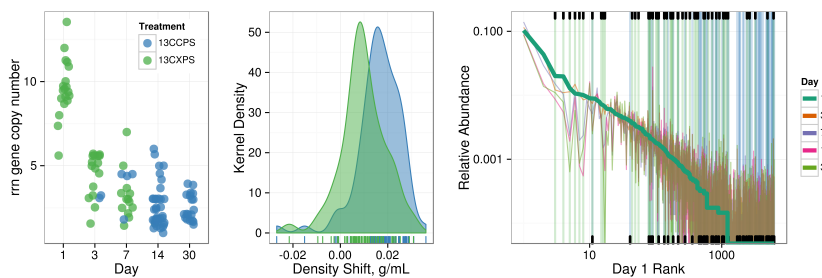


Fig. 4. ^{13}C -responder characteristics based on density shift (A) and rank (B). Kernel density estimation of ^{13}C -responder's density shift in cellulose treatment (blue) and xylose treatment (green) demonstrates degree of labeling for responders for each respective substrate. ^{13}C -responders in rank abundance are labeled by substrate (cellulose, blue; xylose, green). Ticks at top indicate location of ^{13}C -xylose responders in bulk community. Ticks at bottom indicate location of ^{13}C -cellulose responders in bulk community. OTU rank was assessed from day 1 bulk samples.

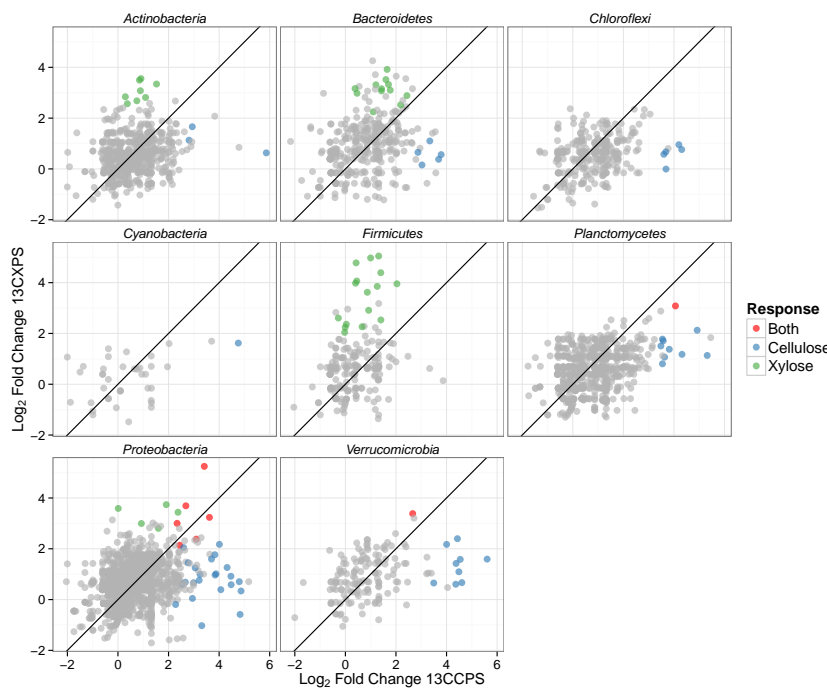


Fig. 5. Maximum log₂ fold change in response to labeled substrate incorporation for each substrate and all OTUs that pass sparsity filtering in both substrate analyses. Points colored by response. Line has slope of 1 with intercept at the origin. OTUs falling in the top-right quadrant responded to both substrates while those in the top-left and bottom-right responded to ¹³C-xylose and ¹³C-cellulose, respectively.

Supplemental Figures and Tables

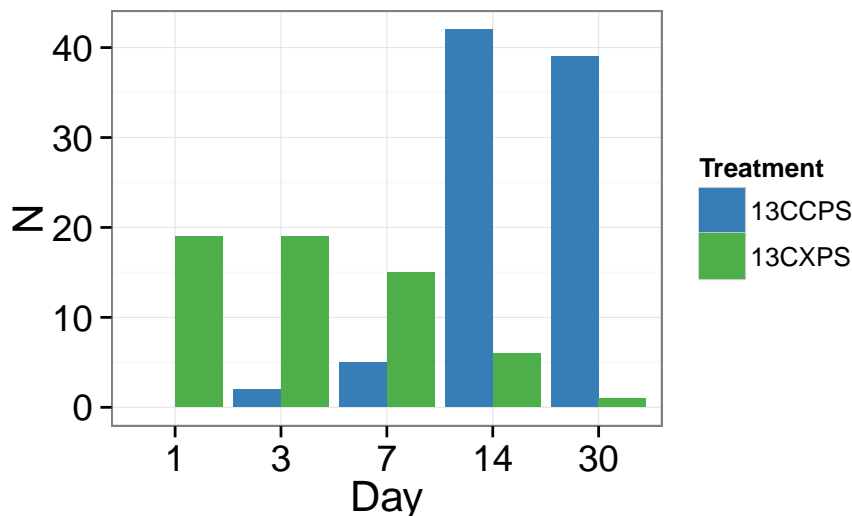


Fig. S1. Counts of responders to each isotopically labeled substrate (cellulose and xylose) over time.

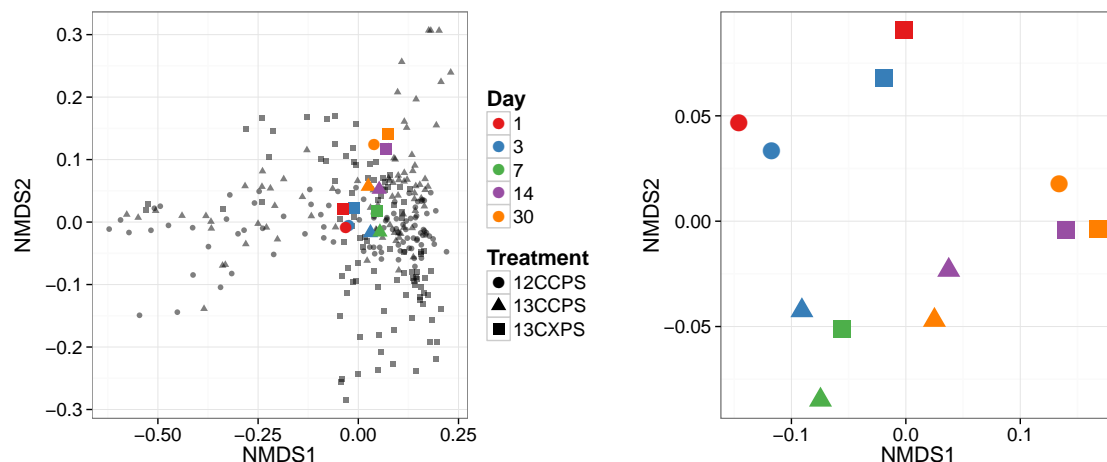


Fig. S2. Ordination of bulk gradient fraction phylogenetic profiles.

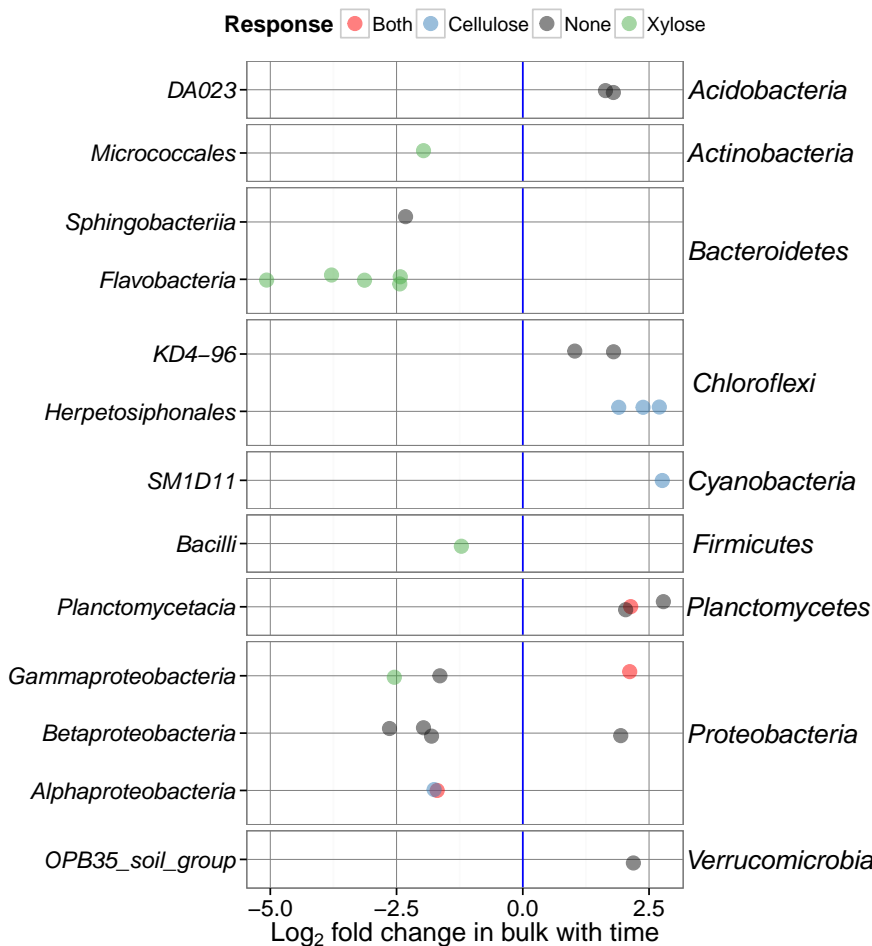


Fig. S3. Fold change time⁻¹ for OTUs that changed significantly in abundance over time. One panel per phylum (phyla indicated on the right). Taxonomic class indicated on the left.

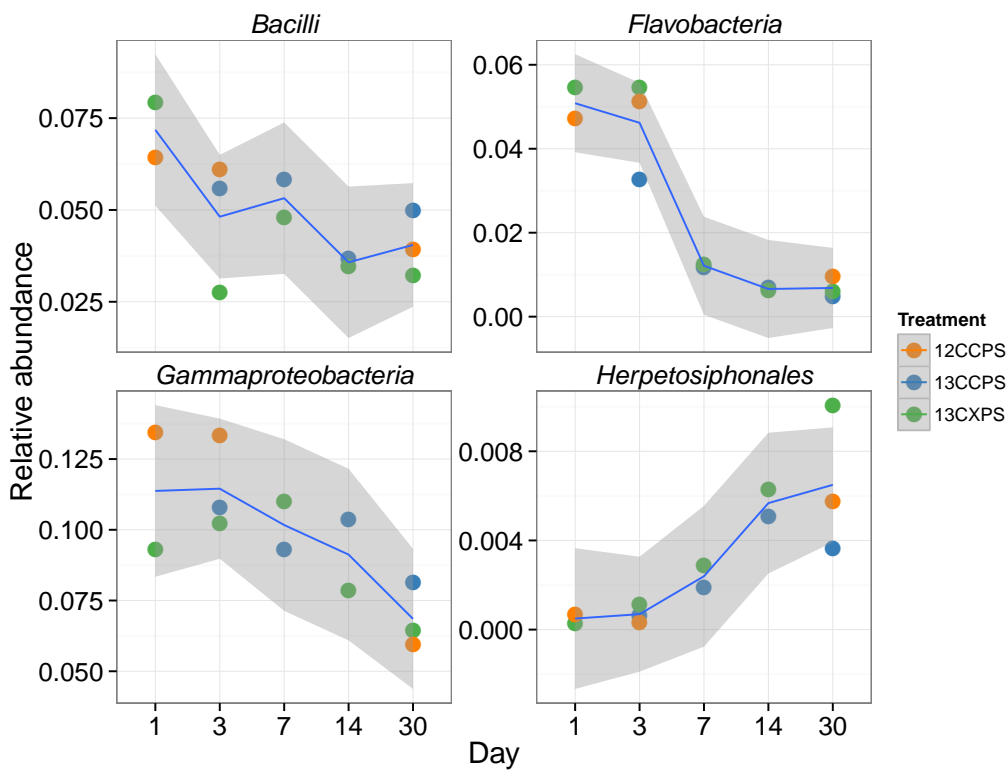


Fig. S4. Relative abundance versus day for classes that changed significantly in relative abundance with time.

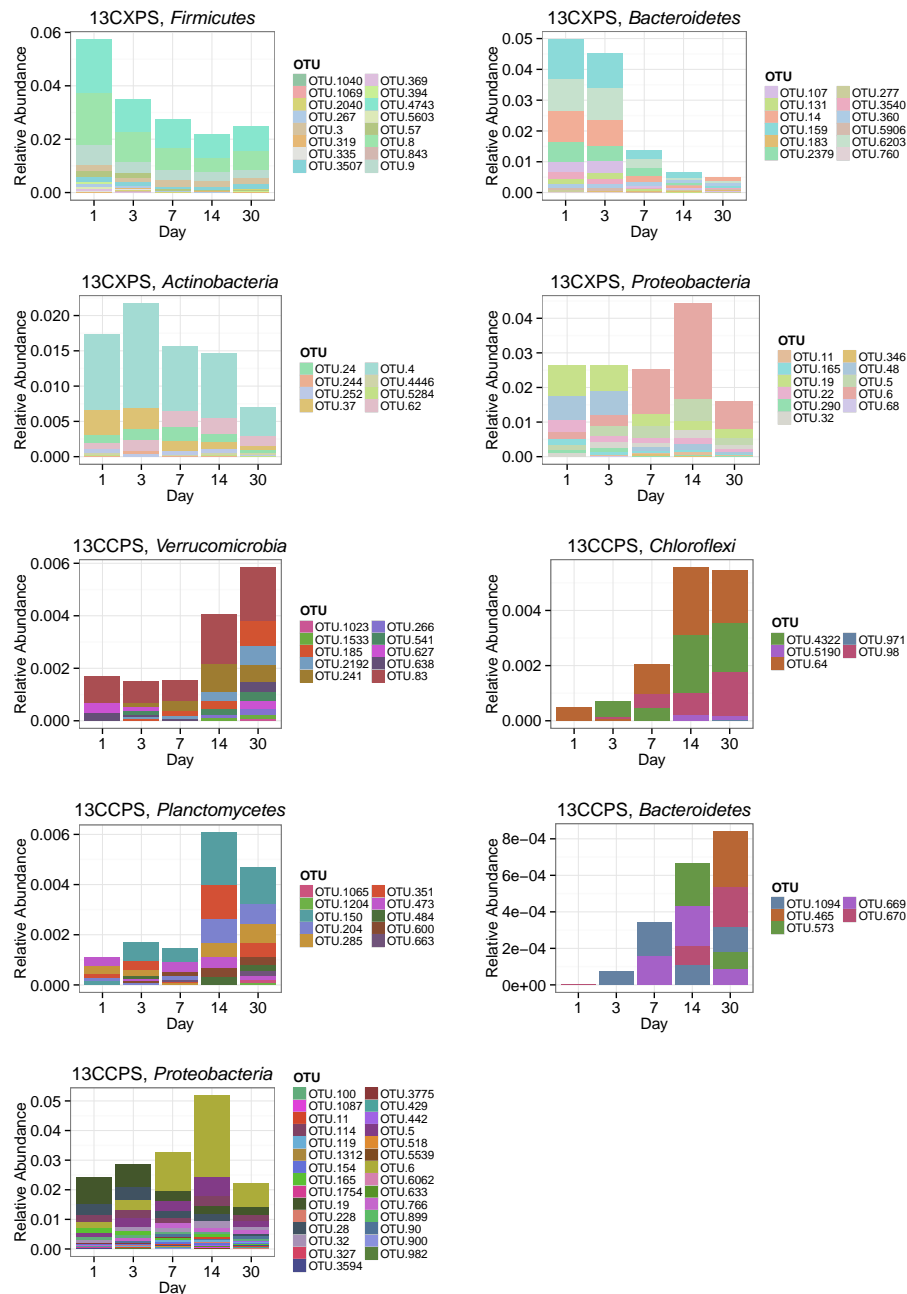


Fig. S5. Sum of bulk abundances with selected phylum for responder OTUs.

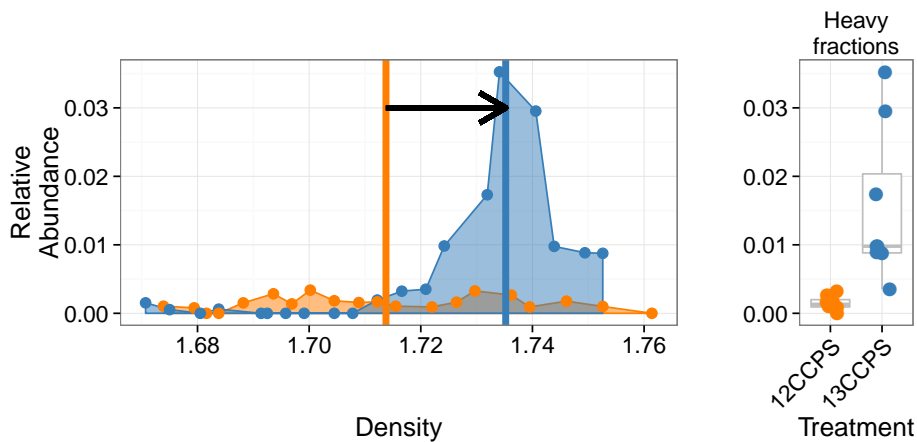


Fig. S6. Density profile for a single ¹³C-cellulose “responder” OTU in the labeled gradient, blue, and the control gradient, orange. Vertical lines show center of mass for each density profile and arrow denotes the magnitude and direction of the BD shift upon labeling. Panel at right shows relative abundance values in the heavy fractions for each gradient.

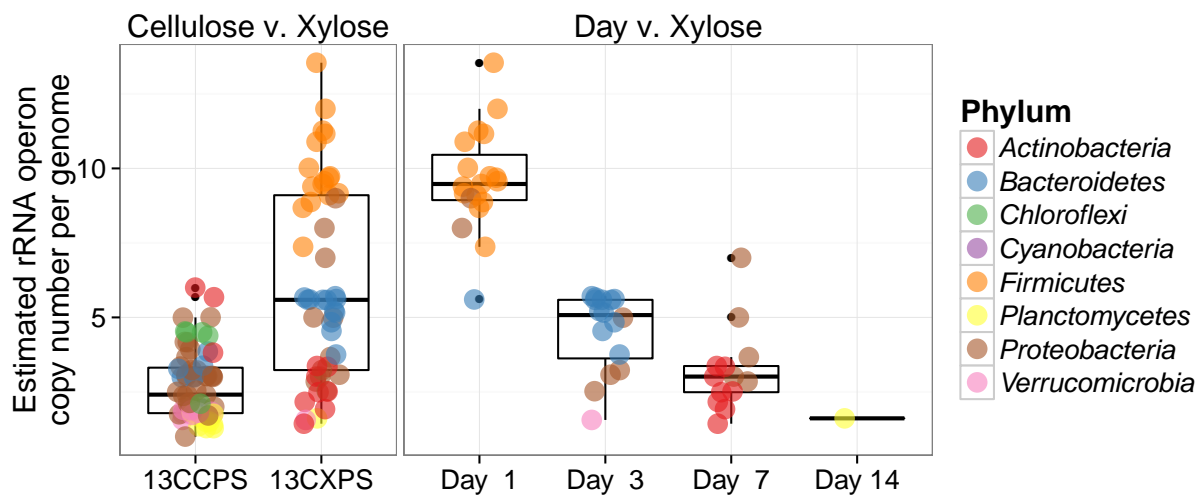


Fig. S7. Estimated rRNA operon copy number per genome for ¹³C responding OTUs. Panel titles indicate which labeled substrate(s) are depicted.

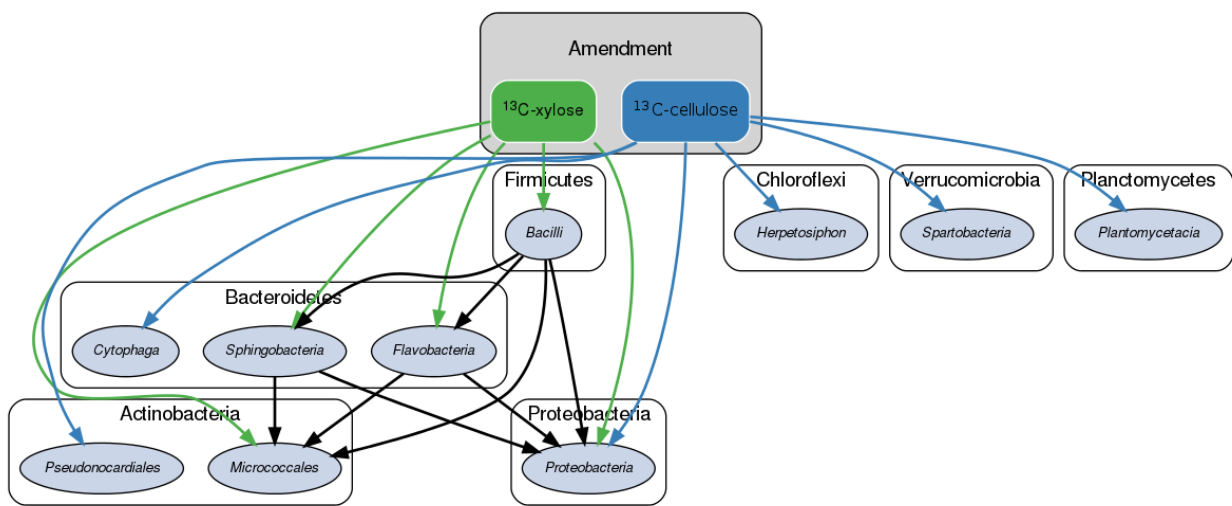


Fig. S8. Conceptual model of soil food web in this experiment.



Fig. S9. Phylum specific trees. Heatmap indicates fold change between heavy fractions of control gradients versus labeled gradients. Dots indicate the position of “responders” to ^{13}C -xylose (green) or ^{13}C -cellulose (blue).

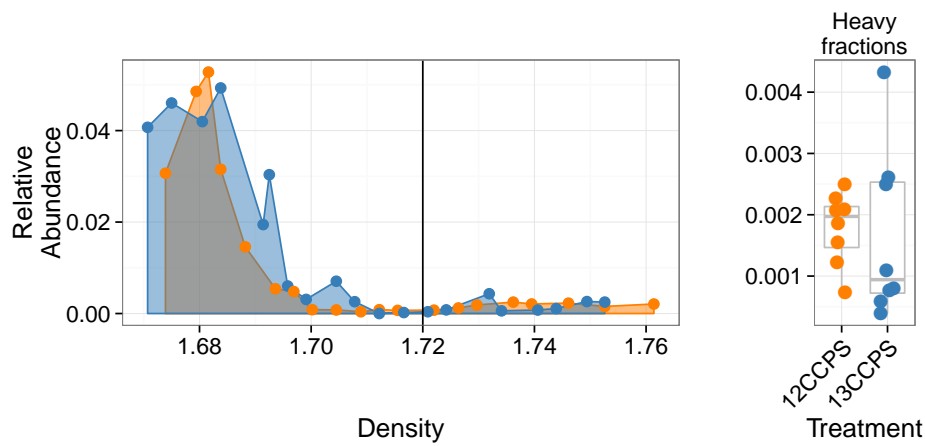


Fig. S10. Density profile for a single ^{13}C -cellulose “non-responder” OTU in the labeled gradient, blue, and the control gradient, orange. Vertical line shows where “heavy” fractions begin as defined in our analysis. Panel at right shows relative abundance values in the heavy fractions for each gradient.

Table S1: ¹³C-cellulose responders BLAST against Living Tree Project

OTU ID	Fold change ^a	Day ^b	Top BLAST hits	BLAST %ID	Phylum;Class;Order
OTU.100	2.66	14	<i>Pseudoxanthomonas sacheonensis</i> , <i>Pseudoxanthomonas dokdonensis</i>	100.0	Proteobacteria Gammaproteobacteria Xanthomonadales
OTU.1023	4.61	30	No hits of at least 90% identity	80.54	Verrucomicrobia Spartobacteria Chthoniobacterales
OTU.1065	5.31	14	No hits of at least 90% identity	84.55	Planctomycetes Planctomycetacia Planctomycetales
OTU.1087	4.32	14	<i>Devsia soli</i> , <i>Devsia crocina</i> , <i>Devsia riboflavina</i>	99.09	Proteobacteria Alphaproteobacteria Rhizobiales
OTU.1094	3.69	30	<i>Sporocytophaga myxococcoides</i>	99.55	Bacteroidetes Cytophagia Cytophagales
OTU.11	3.41	14	<i>Stenotrophomonas pavanii</i> , <i>Stenotrophomonas maltophilia</i> , <i>Pseudomonas geniculata</i>	99.54	Proteobacteria Gammaproteobacteria Xanthomonadales
OTU.114	2.78	14	<i>Herbaspirillum sp. SUEMI03</i> , <i>Herbaspirillum sp. SUEMI10</i> , <i>Oxalicibacterium solurbis</i> , <i>Herminiumonas fonticola</i> , <i>Oxalicibacterium horti</i>	100.0	Proteobacteria Betaproteobacteria Burkholderiales
OTU.119	3.31	14	<i>Brevundimonas alba</i>	100.0	Proteobacteria Alphaproteobacteria Caulobacterales
OTU.120	4.76	14	<i>Vampirovibrio chlorellavorus</i>	94.52	Cyanobacteria SM1D11 uncultured-bacterium
OTU.1204	4.32	30	<i>Planctomyces limnophilus</i>	91.78	Planctomycetes Planctomycetacia Planctomycetales
OTU.1312	4.07	30	<i>Paucimonas lemoignei</i>	99.54	Proteobacteria Betaproteobacteria Burkholderiales
OTU.132	2.81	14	<i>Streptomyces spp.</i>	100.0	Actinobacteria Streptomycetales Streptomycetaceae
OTU.150	4.06	14	No hits of at least 90% identity	86.76	Planctomycetes Planctomycetacia Planctomycetales
OTU.1533	3.43	30	No hits of at least 90% identity	82.27	Verrucomicrobia Spartobacteria Chthoniobacterales
OTU.154	3.24	14	<i>Pseudoxanthomonas mexicana</i> , <i>Pseudoxanthomonas japonensis</i>	100.0	Proteobacteria Gammaproteobacteria Xanthomonadales
OTU.165	3.1	14	<i>Rhizobium skieniewicense</i> , <i>Rhizobium vignae</i> , <i>Rhizobium larrymoorei</i> , <i>Rhizobium alkalisolii</i> , <i>Rhizobium galegae</i> , <i>Rhizobium huautlense</i>	100.0	Proteobacteria Alphaproteobacteria Rhizobiales
OTU.1754	4.48	14	<i>Asticcacaulis biprosthecium</i> , <i>Asticcacaulis benevestitus</i>	96.8	Proteobacteria Alphaproteobacteria Caulobacterales
OTU.185	4.37	14	No hits of at least 90% identity	85.14	Verrucomicrobia Spartobacteria Chthoniobacterales
OTU.19	2.44	14	<i>Rhizobium alamii</i> , <i>Rhizobium mesosinicum</i> , <i>Rhizobium mongolense</i> , <i>Arthrobacter viscosus</i> , <i>Rhizobium sullae</i> , <i>Rhizobium yanglingense</i> , <i>Rhizobium loessense</i>	99.54	Proteobacteria Alphaproteobacteria Rhizobiales
OTU.204	3.81	14	No hits of at least 90% identity	nan	Planctomycetes Planctomycetacia Planctomycetales

Table S1 – continued from previous page

OTU ID	Fold change	Day	Top BLAST hits	BLAST %ID	Phylum;Class;Order
OTU.2192	3.49	30	No hits of at least 90% identity	83.56	Verrucomicrobia Spartobacteria Chthoniobacterales
OTU.228	2.54	30	<i>Sorangium cellulosum</i>	98.17	Proteobacteria Deltaproteobacteria Myxococcales
OTU.241	2.66	14	No hits of at least 90% identity	87.73	Verrucomicrobia Spartobacteria Chthoniobacterales
OTU.257	2.94	14	<i>Lentzea waywayandensis</i> , <i>Lentzea flaviverrucosa</i>	100.0	Actinobacteria Pseudonocardiales Pseudonocardiaceae
OTU.266	4.54	30	No hits of at least 90% identity	83.64	Verrucomicrobia Spartobacteria Chthoniobacterales
OTU.28	2.59	14	<i>Rhizobium giardinii</i> , <i>Rhizobium tubonense</i> , <i>Rhizobium tibeticum</i> , <i>Rhizobium mesoamericanum CCGE 501</i> , <i>Rhizobium herbae</i> , <i>Rhizobium endophyticum</i>	99.54	Proteobacteria Alphaproteobacteria Rhizobiales
OTU.285	3.55	30	<i>Blastopirellula marina</i>	90.87	Planctomycetes Planctomycetacia Planctomycetales
OTU.32	2.34	3	<i>Sandaracinus amylolyticus</i>	94.98	Proteobacteria Deltaproteobacteria Myxococcales
OTU.327	2.99	14	<i>Asticcacaulis biprosthecum</i> , <i>Asticcacaulis benevestitus</i>	98.63	Proteobacteria Alphaproteobacteria Caulobacterales
OTU.351	3.54	14	<i>Pirellula staleyi DSM 6068</i>	91.86	Planctomycetes Planctomycetacia Planctomycetales
OTU.3594	3.83	30	<i>Chondromyces robustus</i>	90.41	Proteobacteria Deltaproteobacteria Myxococcales
OTU.3775	3.88	14	<i>Devosia glacialis</i> , <i>Devosia chinhatensis</i> , <i>Devosia geojensis</i> , <i>Devosia yakushimensis</i>	98.63	Proteobacteria Alphaproteobacteria Rhizobiales
OTU.429	3.7	30	<i>Devosia limi</i> , <i>Devosia psychrophila</i>	97.72	Proteobacteria Alphaproteobacteria Rhizobiales
OTU.4322	4.19	14	No hits of at least 90% identity	89.14	Chloroflexi Herpetosiphonales Herpetosiphonaceae
OTU.442	3.05	30	<i>Chondromyces robustus</i>	92.24	Proteobacteria Deltaproteobacteria Myxococcales
OTU.465	3.79	30	<i>Ohtaekwangia kribbensis</i>	92.73	Bacteroidetes Cytophagia Cytophagales
OTU.473	3.58	14	<i>Pirellula staleyi DSM 6068</i>	90.91	Planctomycetes Planctomycetacia Planctomycetales
OTU.484	4.92	14	No hits of at least 90% identity	89.09	Planctomycetes Planctomycetacia Planctomycetales
OTU.5	2.69	14	<i>Delftia tsuruhatensis</i> , <i>Delftia lacustris</i>	100.0	Proteobacteria Betaproteobacteria Burkholderiales
OTU.518	4.8	14	<i>Hydrogenophaga intermedia</i>	100.0	Proteobacteria Betaproteobacteria Burkholderiales
OTU.5190	3.6	30	No hits of at least 90% identity	88.13	Chloroflexi Herpetosiphonales Herpetosiphonaceae
OTU.541	4.49	30	No hits of at least 90% identity	84.23	Verrucomicrobia Spartobacteria Chthoniobacterales
OTU.5539	4.01	14	<i>Devosia subaequoris</i>	98.17	Proteobacteria Alphaproteobacteria Rhizobiales

Table S1 – continued from previous page

OTU ID	Fold change	Day	Top BLAST hits	BLAST %ID	Phylum;Class;Order
OTU.573	3.03	30	<i>Adhaeribacter aerophilus</i>	92.76	<i>Bacteroidetes Cytophagia Cytophagales</i>
OTU.6	3.62	7	<i>Cellvibrio fulvus</i>	100.0	<i>Proteobacteria Gammaproteobacteria Pseudomonadales</i>
OTU.600	3.48	30	No hits of at least 90% identity	80.37	<i>Planctomycetes Planctomycetacia Planctomycetales</i>
OTU.6062	4.83	30	<i>Dokdonella sp. DC-3, Luteibacter rhizovicinus</i>	97.26	<i>Proteobacteria Gammaproteobacteria Xanthomonadales</i>
OTU.627	4.43	14	<i>Verrucomicrobiaceae bacterium DC2a-G7</i>	100.0	<i>Verrucomicrobia Verrucomicrobiae Verrucomicrobiales</i>
OTU.633	3.84	30	No hits of at least 90% identity	89.5	<i>Proteobacteria Deltaproteobacteria Myxococcales</i>
OTU.638	4.0	30	<i>Luteolibacter sp. CCTCC AB 2010415, Luteolibacter algae</i>	93.61	<i>Verrucomicrobia Verrucomicrobiae Verrucomicrobiales</i>
OTU.64	4.31	14	No hits of at least 90% identity	89.5	<i>Chloroflexi Herpetosiphonales Herpetosiphonaceae</i>
OTU.663	3.63	30	<i>Pirellula staleyi DSM 6068</i>	90.87	<i>Planctomycetes Planctomycetacia Planctomycetales</i>
OTU.669	3.34	30	<i>Ohtaekwangia koreensis</i>	92.69	<i>Bacteroidetes Cytophagia Cytophagales</i>
OTU.670	2.87	30	<i>Adhaeribacter aerophilus</i>	91.78	<i>Bacteroidetes Cytophagia Cytophagales</i>
OTU.766	3.21	14	<i>Devosia insulae</i>	99.54	<i>Proteobacteria Alphaproteobacteria Rhizobiales</i>
OTU.83	5.61	14	<i>Luteolibacter sp. CCTCC AB 2010415</i>	97.72	<i>Verrucomicrobia Verrucomicrobiae Verrucomicrobiales</i>
OTU.862	5.87	14	<i>Allokutzneria albata</i>	100.0	<i>Actinobacteria Pseudonocardiales Pseudonocardiaceae</i>
OTU.899	2.28	30	<i>Enhygromyxa salina</i>	97.72	<i>Proteobacteria Deltaproteobacteria Myxococcales</i>
OTU.90	2.94	14	<i>Sphingopyxis panaciterrae, Sphingopyxis chilensis, Sphingopyxis sp. BZ30, Sphingomonas sp.</i>	100.0	<i>Proteobacteria Alphaproteobacteria Sphingomonadales</i>
OTU.900	4.87	14	<i>Brevundimonas vesicularis, Brevundimonas nasdae</i>	100.0	<i>Proteobacteria Alphaproteobacteria Caulobacterales</i>
OTU.971	3.68	30	No hits of at least 90% identity	78.57	<i>Chloroflexi Anaerolineae Anaerolineales</i>
OTU.98	3.68	14	No hits of at least 90% identity	88.18	<i>Chloroflexi Herpetosiphonales Herpetosiphonaceae</i>
OTU.982	4.47	14	<i>Devosia neptuniae</i>	100.0	<i>Proteobacteria Alphaproteobacteria Rhizobiales</i>

^a Maximum observed \log_2 of fold change.^b Day of maximum fold change.

Table S2: ^{13}C -xylose responders BLAST against Living Tree Project

OTU ID	Fold change ^a	Day ^b	Top BLAST hits	BLAST %ID	Phylum;Class;Order
OTU.1040	4.78	1	<i>Paenibacillus daejeonensis</i>	100.0	<i>Firmicutes Bacilli Bacillales</i>
OTU.1069	3.85	1	<i>Paenibacillus terrigena</i>	100.0	<i>Firmicutes Bacilli Bacillales</i>
OTU.107	2.25	3	<i>Flavobacterium sp. 15C3</i> , <i>Flavobacterium banpakuense</i>	99.54	<i>Bacteroidetes Flavobacteria Flavobacteriales</i>
OTU.11	5.25	7	<i>Stenotrophomonas pavanii</i> , <i>Stenotrophomonas maltophilia</i> , <i>Pseudomonas geniculata</i>	99.54	<i>Proteobacteria Gammaproteobacteria Xanthomonadales</i>
OTU.131	3.07	3	<i>Flavobacterium fluvii</i> , <i>Flavobacterium bacterium HMD1033</i> , <i>Flavobacterium sp. HMD1001</i>	100.0	<i>Bacteroidetes Flavobacteria Flavobacteriales</i>
OTU.14	3.92	3	<i>Flavobacterium oncorhynchi</i> , <i>Flavobacterium glycines</i> , <i>Flavobacterium succinicans</i>	99.09	<i>Bacteroidetes Flavobacteria Flavobacteriales</i>
OTU.150	3.08	14	No hits of at least 90% identity	86.76	<i>Planctomycetes Planctomycetacia Planctomycetales</i>
OTU.159	3.16	3	<i>Flavobacterium hibernum</i>	98.17	<i>Bacteroidetes Flavobacteria Flavobacteriales</i>
OTU.165	2.38	3	<i>Rhizobium skieniewicense</i> , <i>Rhizobium vignae</i> , <i>Rhizobium larrymoorei</i> , <i>Rhizobium alkalisolii</i> , <i>Rhizobium galegae</i> , <i>Rhizobium huautlense</i>	100.0	<i>Proteobacteria Alphaproteobacteria Rhizobiales</i>
OTU.183	3.31	3	No hits of at least 90% identity	89.5	<i>Bacteroidetes Sphingobacteriia Sphingobacteriales</i>
OTU.19	2.14	7	<i>Rhizobium alamii</i> , <i>Rhizobium mesosinicum</i> , <i>Rhizobium mongolense</i> , <i>Arthrobacter viscosus</i> , <i>Rhizobium sullae</i> , <i>Rhizobium yanglingense</i> , <i>Rhizobium loessense</i>	99.54	<i>Proteobacteria Alphaproteobacteria Rhizobiales</i>
OTU.2040	2.91	1	<i>Paenibacillus pectinilyticus</i>	100.0	<i>Firmicutes Bacilli Bacillales</i>
OTU.22	2.8	7	<i>Paracoccus sp. NB88</i>	99.09	<i>Proteobacteria Alphaproteobacteria Rhodobacterales</i>
OTU.2379	3.1	3	<i>Flavobacterium pectinovorum</i> , <i>Flavobacterium sp. CS100</i>	97.72	<i>Bacteroidetes Flavobacteria Flavobacteriales</i>
OTU.24	2.81	7	<i>Cellulomonas aerilata</i> , <i>Cellulomonas humilata</i> , <i>Cellulomonas terrae</i> , <i>Cellulomonas soli</i> , <i>Cellulomonas xylinilytica</i>	100.0	<i>Actinobacteria Micrococcales Cellulomonadaceae</i>
OTU.241	3.38	3	No hits of at least 90% identity	87.73	<i>Verrucomicrobia Spartobacteria Chthoniobacterales</i>
OTU.244	3.08	7	<i>Cellulosimicrobium funkei</i> , <i>Cellulosimicrobium terreum</i>	100.0	<i>Actinobacteria Micrococcales Promicromonosporaceae</i>
OTU.252	3.34	7	<i>Promicromonospora thailandica</i>	100.0	<i>Actinobacteria Micrococcales Promicromonosporaceae</i>
OTU.267	4.97	1	<i>Paenibacillus pabuli</i> , <i>Paenibacillus tundrae</i> , <i>Paenibacillus taichungensis</i> , <i>Paenibacillus xylohexedens</i> , <i>Paenibacillus xylinilyticus</i>	100.0	<i>Firmicutes Bacilli Bacillales</i>
OTU.277	3.52	3	<i>Solibius ginsengiterrae</i>	95.43	<i>Bacteroidetes Sphingobacteriia Sphingobacteriales</i>

Table S2 – continued from previous page

OTU ID	Fold change	Day	Top BLAST hits	BLAST %ID	Phylum;Class;Order
OTU.290	3.59	1	<i>Pantoea spp.</i> , <i>Klugvera spp.</i> , <i>Klebsiella spp.</i> , <i>Erwinia spp.</i> , <i>Enterobacter spp.</i> , <i>Buttiauxella spp.</i>	100.0	Proteobacteria Gammaproteobacteria Enterobacterales
OTU.3	2.61	1	[<i>Brevibacterium</i>] <i>frigoritolerans</i> , <i>Bacillus sp.</i> LMG 20238, <i>Bacillus coahuilensis</i> m4-4, <i>Bacillus simplex</i>	100.0	Firmicutes Bacilli Bacillales
OTU.319	3.98	1	<i>Paenibacillus xinjiangensis</i>	97.25	Firmicutes Bacilli Bacillales
OTU.32	3.0	3	<i>Sandaracinus amyloyticus</i>	94.98	Proteobacteria Deltaproteobacteria Myxococcales
OTU.335	2.53	1	<i>Paenibacillus thailandensis</i>	98.17	Firmicutes Bacilli Bacillales
OTU.346	3.44	3	<i>Pseudoduganella violaceinigra</i>	99.54	Proteobacteria Betaproteobacteria Burkholderiales
OTU.3507	2.36	1	<i>Bacillus spp.</i>	98.63	Firmicutes Bacilli Bacillales
OTU.3540	2.52	3	<i>Flavobacterium terrigena</i>	99.54	Bacteroidetes Flavobacteria Flavobacterales
OTU.360	2.98	3	<i>Flavisolibacter ginsengisoli</i>	95.0	Bacteroidetes Sphingobacteriia Sphingobacterales
OTU.369	5.05	1	<i>Paenibacillus sp.</i> D75, <i>Paenibacillus glycansilyticus</i>	100.0	Firmicutes Bacilli Bacillales
OTU.37	2.68	7	<i>Phycicola gilvus</i> , <i>Microterricola viridarii</i> , <i>Frigeribacterium faeni</i> , <i>Frondihabitans sp.</i> RS-15, <i>Frondihabitans australicus</i>	100.0	Actinobacteria Micrococcales Microbacteriaceae
OTU.394	4.06	1	<i>Paenibacillus pocheonensis</i>	100.0	Firmicutes Bacilli Bacillales
OTU.4	2.84	7	<i>Agromyces ramosus</i>	100.0	Actinobacteria Micrococcales Microbacteriaceae
OTU.4446	3.49	7	<i>Catenuloplanes niger</i> , <i>Catenuloplanes castaneus</i> , <i>Catenuloplanes atrovinosus</i> , <i>Catenuloplanes crispus</i> , <i>Catenuloplanes nepalensis</i> , <i>Catenuloplanes japonicus</i>	97.72	Actinobacteria Frankiales Nakamurellaceae
OTU.4743	2.24	1	<i>Lysinibacillus fusiformis</i> , <i>Lysinibacillus sphaericus</i>	99.09	Firmicutes Bacilli Bacillales
OTU.48	2.99	1	<i>Aeromonas spp.</i>	100.0	Proteobacteria Gammaproteobacteria aaa34a10
OTU.5	3.69	7	<i>Delftia tsuruhatensis</i> , <i>Delftia lacustris</i>	100.0	Proteobacteria Betaproteobacteria Burkholderiales
OTU.5284	3.56	7	<i>Isoptericola nanjingensis</i> , <i>Isoptericola hypogaeus</i> , <i>Isoptericola variabilis</i>	98.63	Actinobacteria Micrococcales Promicromonosporaceae
OTU.5603	3.96	1	<i>Paenibacillus uliginis</i>	100.0	Firmicutes Bacilli Bacillales
OTU.57	4.39	1	<i>Paenibacillus castaneae</i>	98.62	Firmicutes Bacilli Bacillales
OTU.5906	3.16	3	<i>Terrimonas sp.</i> M-8	96.8	Bacteroidetes Sphingobacteriia Sphingobacterales
OTU.6	3.24	3	<i>Cellvibrio fulvus</i>	100.0	Proteobacteria Gammaproteobacteria Pseudomonadales
OTU.62	2.57	7	<i>Nakamurella flava</i>	100.0	Actinobacteria Frankiales Nakamurellaceae

Table S2 – continued from previous page

OTU ID	Fold change	Day	Top BLAST hits	BLAST %ID	Phylum;Class;Order
OTU.6203	3.32	3	<i>Flavobacterium granuli</i> , <i>Flavobacterium glaciei</i>	100.0	<i>Bacteroidetes Flavobacteria Flavobacteriales</i>
OTU.68	3.74	7	<i>Shigella flexneri</i> , <i>Escherichia fergusonii</i> , <i>Escherichia coli</i> , <i>Shigella sonnei</i>	100.0	<i>Proteobacteria Gammaproteobacteria Enterobacteriales</i>
OTU.760	2.89	3	<i>Dyadobacter hamtensis</i>	98.63	<i>Bacteroidetes Cytophagia Cytophagales</i>
OTU.8	2.26	1	<i>Bacillus niaci</i>	100.0	<i>Firmicutes Bacilli Bacillales</i>
OTU.843	3.62	1	<i>Paenibacillus agaragedens</i>	100.0	<i>Firmicutes Bacilli Bacillales</i>
OTU.9	2.04	1	<i>Bacillus megaterium</i> , <i>Bacillus flexus</i>	100.0	<i>Firmicutes Bacilli Bacillales</i>

^a Maximum observed \log_2 of fold change.^b Day of maximum fold change.